11/12/25

Learning Low-Rank Neutron Transport Dynamics on Linear and Nonlinear Manifolds

F. A. B. Silva, J. C. Ragusa

TEXAS A&M UNIVERSITY
Department of Nuclear Engineering

Outline

I. Motivation & Problem Setting

- Why ROM for parametric neutron transport?
- The parametric mono-energetic neutron transport problem
- Full order DG-S_N semi-discretization

II. Methodology

- Linear and Nonlinear Manifold ROM
- Proper orthogonal decomposition
- Nonlinear manifolds via quadratic lifting
- Semi-intrusive operator inference

III. Numerical Results

- 1D slab benchmark – projection & inference
- 1D lifting dimension study
- 2D heterogeneous benchmark – scalar flux & convergence

IV. Conclusions & Future Work

Motivation: UQ in Neutron Transport

Physical Setting

- Time-dependent mono-energetic neutron transport
- Parameter dependent cross sections $\sigma_t(\boldsymbol{\mu})$, $\sigma_s(\boldsymbol{\mu})$ source $Q(t,\boldsymbol{\mu})$, boundary conditions $\Psi^{\text{in}}(\mathbf{x},\boldsymbol{\Omega},t;\boldsymbol{\mu})$

The UQ Challenge

- Epistemic uncertainty: $\boldsymbol{\mu}$ not known exactly
- Need statistics of $\Psi(\mathbf{x},\boldsymbol{\Omega},t;\boldsymbol{\mu})$ or related QoIs
- Monte Carlo / quadrature requires repeated solves

Computational Bottleneck

- A single FOM solve: 10^5–10^9 DOFs, very expensive!
- ROM target: 10^2–$10^5\times$ speed-up at certified accuracy

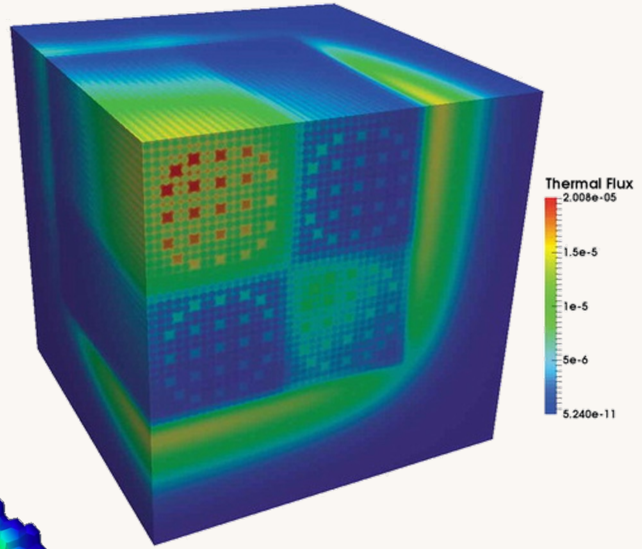

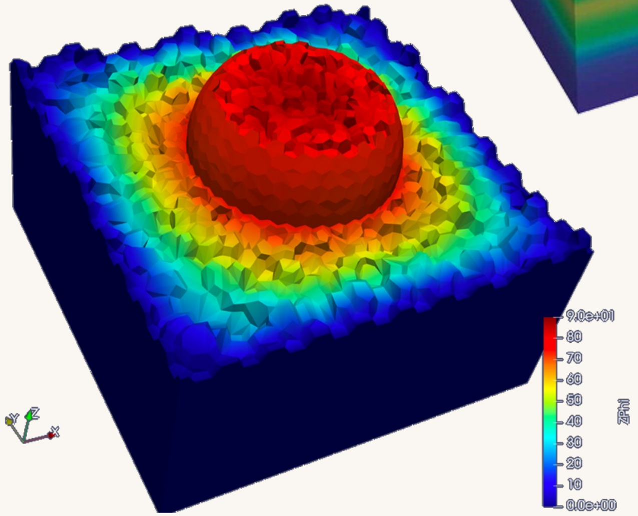

The Parametric Neutron Transport Problem

Strong Form: Find the angular neutron flux $\Psi = \Psi(\mathbf{x}, \boldsymbol{\Omega}, t; \boldsymbol{\mu}): \mathcal{D}\times\mathcal{S}^2\times\mathcal{T}\times\mathcal{U} \to \mathbb{R}$, such that

$$\frac{1}{v}\frac{\partial\Psi}{\partial t} + \boldsymbol{\Omega}\cdot\nabla\Psi + \sigma_t(\boldsymbol{\mu})\Psi - \frac{\sigma_s(\boldsymbol{\mu})}{4\pi}\int_{\mathcal{S}^2}\Psi(\boldsymbol{\Omega}')\mathrm{d}\boldsymbol{\Omega}' = \frac{Q(t,\boldsymbol{\mu})}{4\pi} \qquad \text{in } \mathcal{D}\times\mathcal{S}^2\times\mathcal{T}\times\mathcal{U},$$

$$\Psi(\mathbf{x}, \boldsymbol{\Omega}, t; \boldsymbol{\mu}) = \Psi^{\mathrm{in}}(\mathbf{x}, \boldsymbol{\Omega}, t; \boldsymbol{\mu}) \qquad \text{on } \Gamma^{-}\times\mathcal{T}\times\mathcal{U},$$ *(inflow boundary data)*

$$\Psi(\mathbf{x}, \boldsymbol{\Omega}, 0; \boldsymbol{\mu}) = \Psi_0(\mathbf{x}, \boldsymbol{\Omega}, t; \boldsymbol{\mu}) \qquad \text{on } \mathcal{D}\times\mathcal{S}^2\times\mathcal{T}\times\mathcal{U},$$ *(initial condition)*

Notation:

- $\mathcal{D} \subset \mathbb{R}^3$ compact Lipschitz domain
- $\mathcal{S}^2$ is the unit sphere in $\mathbb{R}^3$ (angle space)
- $\mathcal{T} := [0, \mathrm{T}]$ is the integration time horizon
- $\mathcal{U} \subset \mathbb{R}^{N_\mu}$ is the parameters set
- $v \in \mathbb{R}^+$ is the neutron speed
- $\sigma_t, \sigma_s : \mathcal{D}\times\mathcal{U} \to \mathbb{R}^+$ are heterogeneous macroscopic cross-sections
- $Q : \mathcal{D}\times\mathcal{T}\times\mathcal{U} \to \mathbb{R}$ is a parametric isotropic volumetric source
- $\mathbf{n}(\mathbf{x}) \in \mathcal{S}^2$ is the unit outward normal to $\partial\mathcal{D}$
- $\Gamma^- := \{(\mathbf{x}, \boldsymbol{\Omega}) \in \partial\mathcal{D}\times\mathcal{S}^2 \mid \boldsymbol{\Omega}\cdot\mathbf{n}(\mathbf{x}) < 0\}$ is the inflow boundary

Full-Order Model: DG-S_N Semi-Discretization

Phase-Space Discretization

- S_N angular quadrature: N_Ω discrete directions
- Discontinuous Galerkin (DG) spatial discretization

Monolithic System ODE

$$\mathbb{M}\frac{\mathrm{d}\boldsymbol{\psi}}{\mathrm{d}t} + \left(\mathbb{G} + \mathbb{A}_{\boldsymbol{\mu}} - \mathbb{B}_{\boldsymbol{\mu}}\right)\boldsymbol{\psi} = \boldsymbol{p}_{\boldsymbol{\mu}} + \boldsymbol{q}_{\boldsymbol{\mu}},$$

where:

$\boldsymbol{\psi} \in \mathbb{R}^{\mathcal{N}}$	state vector ($\mathcal{N} = N_\Omega \times N_{\boldsymbol{x}}$ DOFs)
$\mathbb{M} \in \mathbb{R}^{\mathcal{N}\times\mathcal{N}}$	mass matrix
$\mathbb{G} \in \mathbb{R}^{\mathcal{N}\times\mathcal{N}}$	streaming operator (advection)
$\mathbb{A}_{\boldsymbol{\mu}}, \mathbb{B}_{\boldsymbol{\mu}} \in \mathbb{R}^{\mathcal{N}\times\mathcal{N}}$	absorption / scattering operators
$\boldsymbol{p}_{\boldsymbol{\mu}}, \boldsymbol{q}_{\boldsymbol{\mu}} \in \mathbb{R}^{\mathcal{N}}$	volume and boundary sources

Outline

I. Motivation & Problem Setting

- Why ROM for parametric neutron transport?
- The parametric mono-energetic neutron transport problem
- Full order DG-S_N semi-discretization

II. Methodology

- Linear and Nonlinear Manifold ROM
- Proper orthogonal decomposition
- Nonlinear manifolds via quadratic lifting
- Semi-intrusive operator inference

III. Numerical Results

- 1D slab benchmark – projection & inference
- 1D lifting dimension study
- 2D heterogeneous benchmark – scalar flux & convergence

IV. Conclusions & Future Work

Linear vs. Nonlinear Manifold ROM

Linear Manifold (POD-Galerkin)

$\boldsymbol{\psi}(t;\boldsymbol{\mu}) \approx \boldsymbol{\psi}_{\infty}(t) + \mathbb{U}_r \mathbf{c}_r(t;\boldsymbol{\mu})$ with $\mathbb{U}_r \in \mathbb{R}^{\mathcal{N}\times N_r}$

Linear vs. Nonlinear Manifold ROM

Linear Manifold (POD-Galerkin)

$\boldsymbol{\psi}(t;\boldsymbol{\mu}) \approx \boldsymbol{\psi}_\infty(t) + \mathbb{U}_r \mathbf{c}_r(t;\boldsymbol{\mu})$ with $\mathbb{U}_r \in \mathbb{R}^{\mathcal{N}\times N_r}$

ROM via Galerkin projection onto span($\mathbb{U}_r$)

$$\mathbb{M}_r \frac{\mathrm{d}\mathbf{c}_r}{\mathrm{d}t} + \left(\mathbb{G}_r + \mathbb{A}_{\boldsymbol{\mu},r} - \mathbb{B}_{\boldsymbol{\mu},r}\right)\mathbf{c}_r = \boldsymbol{r}_{\boldsymbol{\mu},r}$$

where

$$\mathbb{A}_{\boldsymbol{\mu},r} = \mathbb{U}_r^\top \mathbb{A}_{\boldsymbol{\mu}} \mathbb{U}_r, \qquad \mathbb{M}_r = \mathbb{U}_r^\top \mathbb{M}\ \mathbb{U}_r$$

$$\mathbb{B}_{\boldsymbol{\mu},r} = \mathbb{U}_r^\top \mathbb{B}_{\boldsymbol{\mu}} \mathbb{U}_r, \qquad \mathbb{G}_r = \mathbb{U}_r^\top \mathbb{G}\ \mathbb{U}_r$$

$$\boldsymbol{r}_{\boldsymbol{\mu},r} = \mathbb{U}_r^\top\left(\boldsymbol{p}_{\boldsymbol{\mu}} + \boldsymbol{q}_{\boldsymbol{\mu}} - \left(\mathbb{G} + \mathbb{A}_{\boldsymbol{\mu}} - \mathbb{B}_{\boldsymbol{\mu}}\right)\boldsymbol{\psi}_\infty - \mathbb{M}\frac{\mathrm{d}\boldsymbol{\psi}_\infty}{\mathrm{d}t}\right)$$

Linear vs. Nonlinear Manifold ROM

Linear Manifold (POD-Galerkin)

$\boldsymbol{\psi}(t;\boldsymbol{\mu}) \approx \boldsymbol{\psi}_\infty(t) + \mathbb{U}_r \mathbf{c}_r(t;\boldsymbol{\mu})$ with $\mathbb{U}_r \in \mathbb{R}^{\mathcal{N}\times N_r}$

ROM via Galerkin projection onto span($\mathbb{U}_r$)

$$\mathbb{M}_r \frac{\mathrm{d}\mathbf{c}_r}{\mathrm{d}t} + \left(\mathbb{G}_r + \mathbb{A}_{\boldsymbol{\mu},r} - \mathbb{B}_{\boldsymbol{\mu},r}\right)\mathbf{c}_r = \boldsymbol{r}_{\boldsymbol{\mu},r}$$

where

$$\mathbb{A}_{\boldsymbol{\mu},r} = \mathbb{U}_r^\top \mathbb{A}_{\boldsymbol{\mu}} \mathbb{U}_r, \qquad \mathbb{M}_r = \mathbb{U}_r^\top \mathbb{M}\ \mathbb{U}_r$$

$$\mathbb{B}_{\boldsymbol{\mu},r} = \mathbb{U}_r^\top \mathbb{B}_{\boldsymbol{\mu}} \mathbb{U}_r, \qquad \mathbb{G}_r = \mathbb{U}_r^\top \mathbb{G}\ \mathbb{U}_r$$

$$\boldsymbol{r}_{\boldsymbol{\mu},r} = \mathbb{U}_r^\top\left(\boldsymbol{p}_{\boldsymbol{\mu}} + \boldsymbol{q}_{\boldsymbol{\mu}} - \left(\mathbb{G} + \mathbb{A}_{\boldsymbol{\mu}} - \mathbb{B}_{\boldsymbol{\mu}}\right)\boldsymbol{\psi}_\infty - \mathbb{M}\frac{\mathrm{d}\boldsymbol{\psi}_\infty}{\mathrm{d}t}\right)$$

Nonlinear Manifold (Quadratic Lifting)

$\boldsymbol{\psi}(t;\boldsymbol{\mu}) \approx \boldsymbol{\psi}_\infty(t) + \mathbb{U}_q \mathbf{f}(\mathbf{c}_r(t;\boldsymbol{\mu}))$ with $\mathbb{U}_q = [\mathbb{U}_r, \overline{\mathbb{U}}_q] \in \mathbb{R}^{\mathcal{N}\times(N_r+N_q)}$

assuming quadratic lifting

$\mathbf{f}(\mathbf{c}_r) = [\mathbf{c}_r, \mathbb{X}\,\mathrm{vec}(\mathbf{c}_r\mathbf{c}_r^\top)]^\top \in \mathbb{R}^{N_r+N_q}$

Linear vs. Nonlinear Manifold ROM

Linear Manifold (POD-Galerkin)

$\boldsymbol{\psi}(t;\boldsymbol{\mu}) \approx \boldsymbol{\psi}_\infty(t) + \mathbb{U}_r \mathbf{c}_r(t;\boldsymbol{\mu})$ with $\mathbb{U}_r \in \mathbb{R}^{\mathcal{N}\times N_r}$

ROM via Galerkin projection onto span($\mathbb{U}_r$)

$$\mathbb{M}_r \frac{\mathrm{d}\mathbf{c}_r}{\mathrm{d}t} + \left(\mathbb{G}_r + \mathbb{A}_{\boldsymbol{\mu},r} - \mathbb{B}_{\boldsymbol{\mu},r}\right)\mathbf{c}_r = \boldsymbol{r}_{\boldsymbol{\mu},r}$$

where

$$\mathbb{A}_{\boldsymbol{\mu},r} = \mathbb{U}_r^\top \mathbb{A}_{\boldsymbol{\mu}} \mathbb{U}_r, \qquad \mathbb{M}_r = \mathbb{U}_r^\top \mathbb{M}\ \mathbb{U}_r$$

$$\mathbb{B}_{\boldsymbol{\mu},r} = \mathbb{U}_r^\top \mathbb{B}_{\boldsymbol{\mu}} \mathbb{U}_r, \qquad \mathbb{G}_r = \mathbb{U}_r^\top \mathbb{G}\ \mathbb{U}_r$$

$$\boldsymbol{r}_{\boldsymbol{\mu},r} = \mathbb{U}_r^\top\left(\boldsymbol{p}_{\boldsymbol{\mu}} + \boldsymbol{q}_{\boldsymbol{\mu}} - \left(\mathbb{G} + \mathbb{A}_{\boldsymbol{\mu}} - \mathbb{B}_{\boldsymbol{\mu}}\right)\boldsymbol{\psi}_\infty - \mathbb{M}\frac{\mathrm{d}\boldsymbol{\psi}_\infty}{\mathrm{d}t}\right)$$

Nonlinear Manifold (Quadratic Lifting)

$\boldsymbol{\psi}(t;\boldsymbol{\mu}) \approx \boldsymbol{\psi}_\infty(t) + \mathbb{U}_q \mathbf{f}(\mathbf{c}_r(t;\boldsymbol{\mu}))$ with $\mathbb{U}_q = [\mathbb{U}_r, \overline{\mathbb{U}}_q] \in \mathbb{R}^{\mathcal{N}\times(N_r+N_q)}$

assuming quadratic lifting

$\mathbf{f}(\mathbf{c}_r) = [\mathbf{c}_r, \mathbb{X}\,\mathrm{vec}(\mathbf{c}_r\mathbf{c}_r^\top)]^\top \in \mathbb{R}^{N_r+N_q}$

ROM via projection onto span($\mathbb{U}_r$) and reconstruction on span($\mathbb{U}_q$)

$$\mathbb{M}_r \frac{\mathrm{d}\mathbf{c}_r}{\mathrm{d}t} + \left(\mathbb{G}_r + \mathbb{A}_{\boldsymbol{\mu},r} - \mathbb{B}_{\boldsymbol{\mu},r}\right)\mathbf{c}_r + \left(\overline{\mathbb{G}}_r + \overline{\mathbb{A}}_{\boldsymbol{\mu},r} - \overline{\mathbb{B}}_{\boldsymbol{\mu},r}\right)\mathbb{X}\,\mathrm{vec}(\mathbf{c}_r\mathbf{c}_r^\top) = \boldsymbol{r}_{\boldsymbol{\mu},r}$$

where

$$\overline{\mathbb{A}}_{\boldsymbol{\mu},r} = \mathbb{U}_r^\top \mathbb{A}_{\boldsymbol{\mu}} \overline{\mathbb{U}}_q, \qquad \mathbf{0} = \mathbb{U}_r^\top \mathbb{M}\,\overline{\mathbb{U}}_q$$

$$\overline{\mathbb{B}}_{\boldsymbol{\mu},r} = \mathbb{U}_r^\top \mathbb{B}_{\boldsymbol{\mu}} \overline{\mathbb{U}}_q, \qquad \overline{\mathbb{G}}_r = \mathbb{U}_r^\top \mathbb{G}\,\overline{\mathbb{U}}_q$$

Linear vs. Nonlinear Manifold ROM

Linear Manifold (POD-Galerkin)

$\boldsymbol{\psi}(t;\boldsymbol{\mu}) \approx \boldsymbol{\psi}_\infty(t) + \mathbb{U}_r \mathbf{c}_r(t;\boldsymbol{\mu})$ with $\mathbb{U}_r \in \mathbb{R}^{\mathcal{N}\times N_r}$

Nonlinear Manifold (Quadratic Lifting)

$\boldsymbol{\psi}(t;\boldsymbol{\mu}) \approx \boldsymbol{\psi}_\infty(t) + \mathbb{U}_q \mathbf{f}(\mathbf{c}_r(t;\boldsymbol{\mu}))$ with $\mathbb{U}_q = [\mathbb{U}_r, \overline{\mathbb{U}}_q] \in \mathbb{R}^{\mathcal{N}\times(N_r+N_q)}$

assuming quadratic lifting

$\mathbf{f}(\mathbf{c}_r) = [\mathbf{c}_r, \mathbb{X}\,\mathrm{vec}(\mathbf{c}_r\mathbf{c}_r^\top)]^\top \in \mathbb{R}^{N_r+N_q}$

Why Standard ROMs Struggle

- Slow Kolmogorov n-width decay for transport
- No global assemblage of the matrix $\mathbb{G}$

Linear vs. Nonlinear Manifold ROM

Linear Manifold (POD-Galerkin)

$\boldsymbol{\psi}(t;\boldsymbol{\mu}) \approx \boldsymbol{\psi}_\infty(t) + \mathbb{U}_r \mathbf{c}_r(t;\boldsymbol{\mu})$ with $\mathbb{U}_r \in \mathbb{R}^{\mathcal{N}\times N_r}$

Nonlinear Manifold (Quadratic Lifting)

$\boldsymbol{\psi}(t;\boldsymbol{\mu}) \approx \boldsymbol{\psi}_\infty(t) + \mathbb{U}_q \mathbf{f}(\mathbf{c}_r(t;\boldsymbol{\mu}))$ with $\mathbb{U}_q = [\mathbb{U}_r, \overline{\mathbb{U}}_q] \in \mathbb{R}^{\mathcal{N}\times(N_r+N_q)}$

assuming quadratic lifting

$\mathbf{f}(\mathbf{c}_r) = [\mathbf{c}_r, \mathbb{X}\,\mathrm{vec}(\mathbf{c}_r\mathbf{c}_r^\top)]^\top \in \mathbb{R}^{N_r+N_q}$

Why Standard ROMs Struggle

- Slow Kolmogorov n-width decay for transport
- No global assemblage of the matrix $\mathbb{G}$

Our Approach

- Nonlinear manifold to overcome slow n-width decay
- Semi-intrusive inference to avoid global $\mathbb{G}$ assembly
- Projection based assemblage of the affine-decomposed operators $\mathbb{A}_{\boldsymbol{\mu}}, \mathbb{B}_{\boldsymbol{\mu}}$ and of the vector $\boldsymbol{p}_{\boldsymbol{\mu}}, \boldsymbol{q}_{\boldsymbol{\mu}}$.

Training Phase: A Three-steps Approach

1) Reduced Basis Space (offline)

- Collect N_S snapshots $\boldsymbol{\psi}(t_i; \boldsymbol{\mu}_i)$ from the full order model
- Compute POD basis $\mathbb{U}_q = [\mathbb{U}_r, \overline{\mathbb{U}}_q] \in \mathbb{R}^{\mathcal{N}\times(N_r+N_q)}$ truncated at relative energy threshold $\varepsilon > 0$

2) Nonlinear Manifold (offline)

- Choose a nonlinear function, $\mathbf{f}(\mathbf{c}_r) = [\mathbf{c}_r, \mathbb{X}\,\mathrm{vec}(\mathbf{c}_r\mathbf{c}_r^\top)]^\top$ (N_r latent variables, N_p lifting coordinates)
- Identify the lifting coefficients matrix $\mathbb{X}$ via Tikhonov-regularized least squares

3) Operator Inference (offline)

- Compute the reduced reaction operators $\mathbb{A}_{\boldsymbol{\mu},r}, \overline{\mathbb{A}}_{\boldsymbol{\mu},r}$, and $\mathbb{B}_{\boldsymbol{\mu},r}, \overline{\mathbb{B}}_{\boldsymbol{\mu},r}$ via direct projection from cell-local data
- Use alternating minimization to infer the nonlinear pair $\mathbb{G}_r$, $\overline{\mathbb{G}}_r$.

Proper Orthogonal Decomposition

Snapshot matrix

- Center snapshots: $\boldsymbol{s}^{(i)} = \boldsymbol{\psi}(t_i; \boldsymbol{\mu}_i) - \boldsymbol{\psi}_\infty(t_i)$
- Build snapshot matrix: $\mathbb{S} = \left[\boldsymbol{s}^{(1)}, \cdots, \boldsymbol{s}^{(N_S)}\right] \in \mathbb{R}^{\mathcal{N} \times N_S}$

Thin SVD and truncation

- Compute: $\mathbb{M}^{1/2}\mathbb{S} = \breve{\mathbb{U}}\Sigma\mathbb{V}^\top,\ \sigma_1 \geq \cdots \geq \sigma_{N_S} \geq 0$
- Retain $N_r + N_q$ leading modes at energy threshold $\varepsilon > 0$
- Augmented POD basis: $\mathbb{M}^{-\frac{1}{2}}\breve{\mathbb{U}}_q = \left[\mathbb{U}_r, \overline{\mathbb{U}}_q\right] \in \mathbb{R}^{\mathcal{N} \times (N_r + N_q)}$
- Orthogonal components: $\mathbb{U}_r^\top \mathbb{M} \overline{\mathbb{U}}_q = \mathbf{0}$

Latent and lifting coordinates

- Latent coords: $\mathbf{c}_r = \mathbb{U}_r^\top \boldsymbol{s} \in \mathbb{R}^{N_r}$
- Lifting coords: $\bar{\mathbf{c}}_q = \overline{\mathbb{U}}_q^\top \boldsymbol{s} \in \mathbb{R}^{N_q}$

Nonlinear Manifold Learning

Quadratic approximation

- POD residual: $\boldsymbol{s}^{(i)} - \mathbb{U}_r \mathbf{c}_r^{(i)} \approx \overline{\mathbb{U}}_q \bar{\mathbf{c}}_q^{(i)}$
- Quadratic ansatz: $\boldsymbol{s}^{(i)} - \mathbb{U}_r \mathbf{c}_r^{(i)} \approx \overline{\mathbb{U}}_q \mathbb{X}\, \mathrm{vec}(\mathbf{c}_r^{(i)} \mathbf{c}_r^{(i)\top})$

Tikhonov regularized least squares

Estimate the coefficient matrix $\mathbb{X} \in \mathbb{R}^{N_q \times N_r^2}$ by solving

the minimization problem

$$\mathbb{X} = \mathbb{Y}\mathbb{L} \quad \text{with} \quad \mathbb{Y} = \underset{\breve{\mathbb{Y}}}{\arg\min} \sum_{i=1}^{N_S} \left\| \breve{\mathbb{Y}}\mathbb{L}\mathrm{vec}(\mathbf{c}_r^{(i)} \mathbf{c}_r^{(i)\top}) - \bar{\mathbf{c}}_q^{(i)} \right\|^2 + \gamma \left\| \breve{\mathbb{Y}} \right\|^2$$

Where we have introduced the structure matrix $\mathbb{L} \in \mathbb{R}^{N_\ell \times N_r^2}$,
and the unknowns' matrix $\mathbb{Y} \in \mathbb{R}^{N_q \times N_\ell}$.

Nonlinear Manifold Learning

Quadratic approximation

- POD residual: $\boldsymbol{s}^{(i)} - \mathbb{U}_r \mathbf{c}_r^{(i)} \approx \overline{\mathbb{U}}_q \bar{\mathbf{c}}_q^{(i)}$
- Quadratic ansatz: $\boldsymbol{s}^{(i)} - \mathbb{U}_r \mathbf{c}_r^{(i)} \approx \overline{\mathbb{U}}_q \mathbb{X}\, \mathrm{vec}(\mathbf{c}_r^{(i)} \mathbf{c}_r^{(i)\top})$

Tikhonov regularized least squares

Estimate the coefficient matrix $\mathbb{X} \in \mathbb{R}^{N_q \times N_r^2}$ by solving the minimization problem

$$\mathbb{X} = \mathbb{Y}\mathbb{L} \quad \text{with} \quad \mathbb{Y} = \underset{\breve{\mathbb{Y}}}{\arg\min} \sum_{i=1}^{N_S} \left\| \breve{\mathbb{Y}}\mathbb{L}\mathrm{vec}(\mathbf{c}_r^{(i)} \mathbf{c}_r^{(i)\top}) - \bar{\mathbf{c}}_q^{(i)} \right\|^2 + \gamma \left\| \breve{\mathbb{Y}} \right\|^2$$

Where we have introduced the structure matrix $\mathbb{L} \in \mathbb{R}^{N_\ell \times N_r^2}$, and the unknowns' matrix $\mathbb{Y} \in \mathbb{R}^{N_q \times N_\ell}$.

Two variations for $\mathbb{L}$

- **Tensorial**: $\mathbb{L} \in \mathbb{R}^{N_r(N_r+1)/2 \times N_r^2}$, $N_\ell = N_r(N_r+1)/2$, captures all pairwise mode interactions
- **Element-wise quadratic**: $\mathbb{L} \in \mathbb{R}^{N_r/2 \times N_r^2}$, $N_\ell = N_r$, captures only the independent quadratic terms

Notice that $\mathbb{X}$ is computed once offline from snapshot data alone.

Semi-Intrusive Operator Inference

Projected (Intrusive) Operators

- Reaction operator projection requires no global assembly: exploit cell-local structure of DG

$$\mathbb{M}_r \frac{\mathrm{d}\mathbf{c}_r}{\mathrm{d}t} + \left(\mathbb{G}_r + \mathbb{A}_{\boldsymbol{\mu},r} - \mathbb{B}_{\boldsymbol{\mu},r}\right)\mathbf{c}_r + \left(\overline{\mathbb{G}}_r + \overline{\mathbb{A}}_{\boldsymbol{\mu},r} - \overline{\mathbb{B}}_{\boldsymbol{\mu},r}\right)\mathbb{X}\,\mathrm{vec}(\mathbf{c}_r\mathbf{c}_r^\top) = \boldsymbol{r}_{\boldsymbol{\mu},r}$$

Semi-Intrusive Operator Inference

Projected (Intrusive) Operators

- Reaction operator projection requires no global assembly: exploit cell-local structure of DG
- Streaming $\mathbb{G}$ cannot be accessed directly (non-symmetric, element-coupling)

$$\mathbb{M}_r \frac{\mathrm{d}\mathbf{c}_r}{\mathrm{d}t} + \left(\mathbb{G}_r + \mathbb{A}_{\boldsymbol{\mu},r} - \mathbb{B}_{\boldsymbol{\mu},r}\right)\mathbf{c}_r + \left(\overline{\mathbb{G}}_r + \overline{\mathbb{A}}_{\boldsymbol{\mu},r} - \overline{\mathbb{B}}_{\boldsymbol{\mu},r}\right)\mathbb{X}\,\mathrm{vec}(\mathbf{c}_r\mathbf{c}_r^\top) = \boldsymbol{r}_{\boldsymbol{\mu},r}$$

Semi-Intrusive Operator Inference

Projected (Intrusive) Operators

- Reaction operator projection requires no global assembly: exploit cell-local structure of DG
- Streaming $\mathbb{G}$ cannot be accessed directly (non-symmetric, element-coupling)

$$\mathbb{M}_r \frac{\mathrm{d}\mathbf{c}_r}{\mathrm{d}t} + \left(\mathbb{G}_r + \mathbb{A}_{\boldsymbol{\mu},r} - \mathbb{B}_{\boldsymbol{\mu},r}\right)\mathbf{c}_r + \left(\bar{\mathbb{G}}_r + \bar{\mathbb{A}}_{\boldsymbol{\mu},r} - \bar{\mathbb{B}}_{\boldsymbol{\mu},r}\right)\mathbb{X}\,\mathrm{vec}(\mathbf{c}_r\mathbf{c}_r^\top) = \boldsymbol{r}_{\boldsymbol{\mu},r}$$

Operator Inference (Linear Case)

- Residual formulation from snapshot data:

$$\mathbb{G}_r \boldsymbol{c}_r^{(i)} = \boldsymbol{r}_{\boldsymbol{\mu}_i,r} - \left(\mathbb{A}_{\boldsymbol{\mu}_i,r} - \mathbb{B}_{\boldsymbol{\mu}_i,r}\right)\boldsymbol{c}_r^{(i)} - \mathbb{M}_r \frac{\mathrm{d}\mathbf{c}_r^{(i)}}{\mathrm{d}t} = \boldsymbol{g}_r^{(i)}$$

$$\boldsymbol{c}_r^{(i)} = \mathbb{U}_r^\top \boldsymbol{s}(t_i; \boldsymbol{\mu}_i)$$

- Tikhonov regularized least squares over all snapshots

$$\mathbb{G}_r = \underset{\breve{\mathbb{G}}_r}{\arg\min} \sum_{i=1}^{N_S} \left\| \breve{\mathbb{G}}_r \boldsymbol{c}_r^{(i)} - \boldsymbol{g}_r^{(i)} \right\|^2 + \lambda_{\mathrm{L}} \left\| \breve{\mathbb{G}}_r \right\|^2$$

Semi-Intrusive Operator Inference

Projected (Intrusive) Operators

- Reaction operator projection requires no global assembly: exploit cell-local structure of DG
- Streaming $\mathbb{G}$ cannot be accessed directly (non-symmetric, element-coupling)

$$\mathbb{M}_r \frac{\mathrm{d}\mathbf{c}_r}{\mathrm{d}t} + \left(\mathbb{G}_r + \mathbb{A}_{\boldsymbol{\mu},r} - \mathbb{B}_{\boldsymbol{\mu},r}\right)\mathbf{c}_r + \left(\overline{\mathbb{G}}_r + \overline{\mathbb{A}}_{\boldsymbol{\mu},r} - \overline{\mathbb{B}}_{\boldsymbol{\mu},r}\right)\mathbb{X}\,\mathrm{vec}(\mathbf{c}_r\mathbf{c}_r^\top) = \boldsymbol{r}_{\boldsymbol{\mu},r}$$

Operator Inference (Linear Case)

- Residual formulation from snapshot data:

$$\mathbb{G}_r \boldsymbol{c}_r^{(i)} = \boldsymbol{r}_{\boldsymbol{\mu}_i,r} - \left(\mathbb{A}_{\boldsymbol{\mu}_i,r} - \mathbb{B}_{\boldsymbol{\mu}_i,r}\right)\boldsymbol{c}_r^{(i)} - \mathbb{M}_r \frac{\mathrm{d}\mathbf{c}_r^{(i)}}{\mathrm{d}t} = \boldsymbol{g}_r^{(i)}$$

$$\boldsymbol{c}_r^{(i)} = \mathbb{U}_r^\top \boldsymbol{s}(t_i;\boldsymbol{\mu}_i)$$

- Tikhonov regularized least squares over all snapshots

$$\mathbb{G}_r = \arg\min_{\breve{\mathbb{G}}_r} \sum_{i=1}^{N_S} \left\|\breve{\mathbb{G}}_r \boldsymbol{c}_r^{(i)} - \boldsymbol{g}_r^{(i)}\right\|^2 + \lambda_{\mathrm{L}}\left\|\breve{\mathbb{G}}_r\right\|^2$$

Operator Inference (Nonlinear Case)

- Lifted ROM model:

$$\mathbb{G}_r \boldsymbol{c}_r^{(i)} + \overline{\mathbb{G}}_r \mathbb{X}\,\mathrm{vec}(\mathbf{c}_r^{(i)}\mathbf{c}_r^{(i)\top})$$
$$= \boldsymbol{r}_{\boldsymbol{\mu}_i,r} - \left(\mathbb{A}_{\boldsymbol{\mu}_i,r} - \mathbb{B}_{\boldsymbol{\mu}_i,r}\right)\boldsymbol{c}_r^{(i)} - \left(\overline{\mathbb{A}}_{\boldsymbol{\mu}_i,r} - \overline{\mathbb{B}}_{\boldsymbol{\mu}_i,r}\right)\mathbb{X}\,\mathrm{vec}\left(\mathbf{c}_r^{(i)}\mathbf{c}_r^{(i)\top}\right) - \mathbb{M}_r \frac{\mathrm{d}\mathbf{c}_r^{(i)}}{\mathrm{d}t}$$

- Alternating minimization:

  i. Fix $\overline{\mathbb{G}}_r$, solve for $\mathbb{G}_r$ by least squares (λ_{L} regularization)

  ii. Fix $\mathbb{G}_r$, solve for $\overline{\mathbb{G}}_r$ by least squares (λ_{H} regularization)

  Repeat until convergence

Outline

I. Motivation & Problem Setting

- Why ROM for parametric neutron transport?
- The parametric mono-energetic neutron transport problem
- Full order DG-S_N semi-discretization

II. Methodology

- Linear and Nonlinear Manifold ROM
- Proper orthogonal decomposition
- Nonlinear manifolds via quadratic lifting
- Semi-intrusive operator inference

III. Numerical Results

- 1D slab benchmark – projection & inference
- 1D lifting dimension study
- 2D heterogeneous benchmark – scalar flux & convergence

IV. Conclusions & Future Work

1D Slab Benchmark

1D Slab Configuration

- Domain: $\mathcal{D} = [0, 3]$
- Scattering ratio: $\sigma_s/\sigma_t = 0.99$ (highly scattering)
- S_N quadrature: $N_\Omega = 4$ angles
- DG spatial: $N_x = 1{,}500$ cells
- Total DOF: $\mathcal{N} = 6{,}000$
- Time horizon: $T = 10$, $N_S = 7{,}501$ snapshots

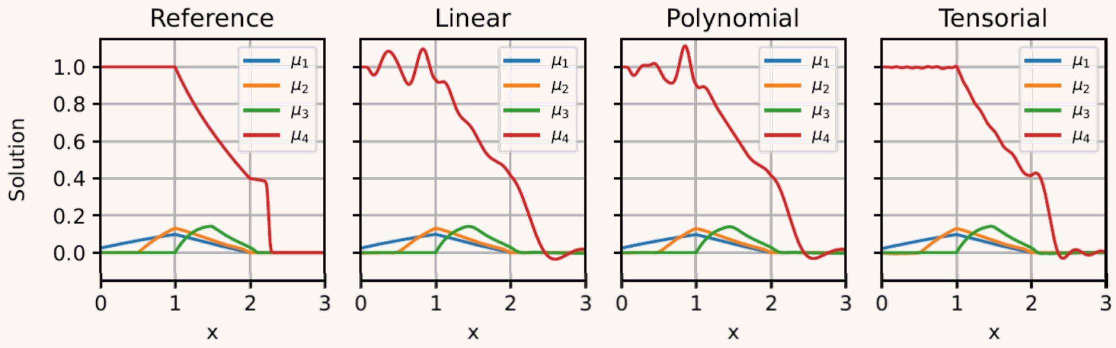

1D Slab Benchmark

1D Slab Configuration

- Domain: $\mathcal{D} = [0, 3]$
- Scattering ratio: $\sigma_s/\sigma_t = 0.99$ (highly scattering)
- S_N quadrature: $N_\Omega = 4$ angles
- DG spatial: $N_x = 1{,}500$ cells
- Total DOF: $\mathcal{N} = 6{,}000$
- Time horizon: $T = 10$, $N_S = 7{,}501$ snapshots

ROM Configuration

- Latent dimension: $N_r = 16$
- Lifting dimension: $N_q = 548$
- Models tested: Linear, Element-wise, Tensorial
- Intrusive (projected) vs Semi-intrusive (inferred)

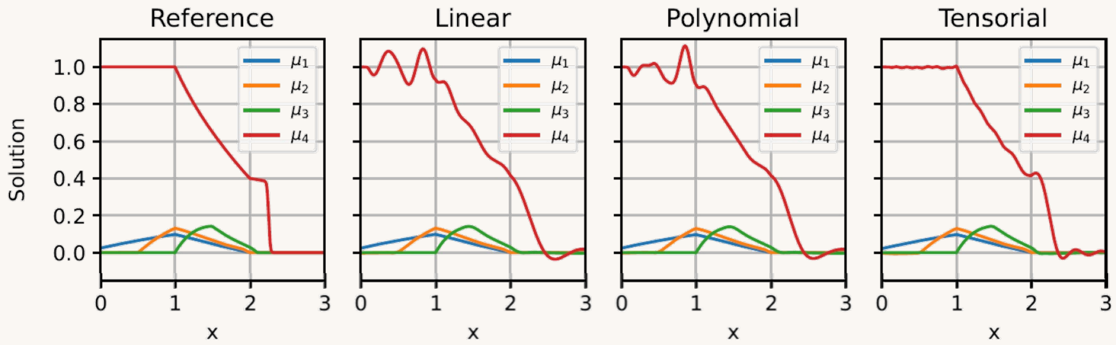

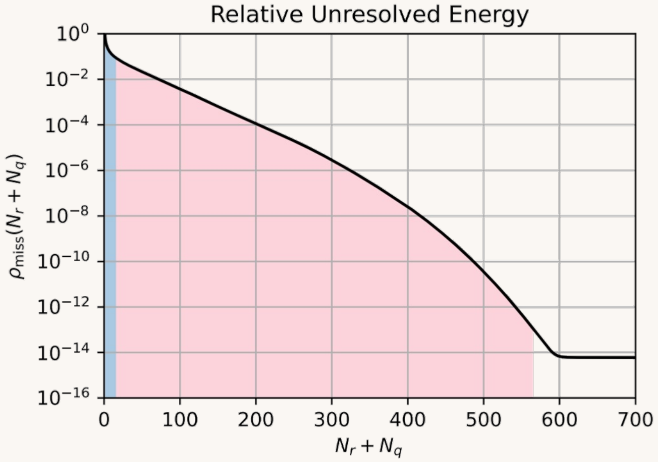

1D Results

Projection-Based (Intrusive) ROM

- Tensorial model achieves lowest $L^2(\mathcal{D}\times\mathcal{S}^2)$ error
- Element-wise ≈ Linear: polynomial structure insufficient
- All models stable over full time interval $\mathcal{T} = [0, T]$

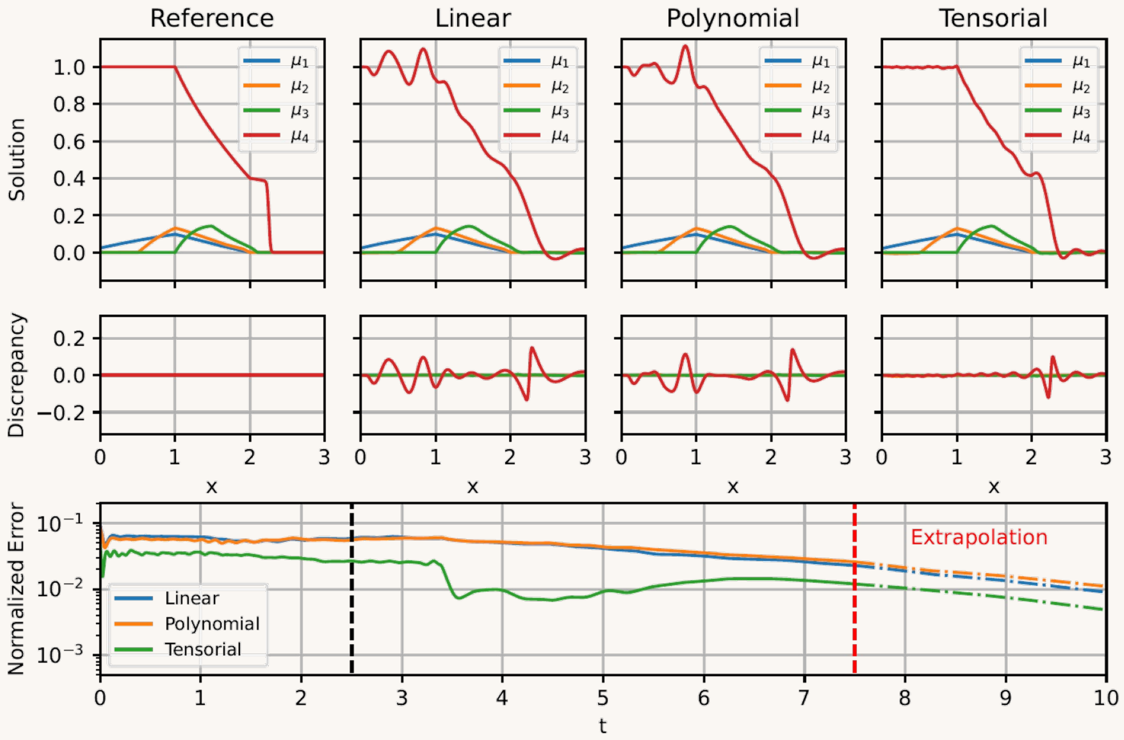

1D Results

Projection-Based (Intrusive) ROM

- Tensorial model achieves lowest $L^2(\mathcal{D}\times\mathcal{S}^2)$ error
- Element-wise ≈ Linear: polynomial structure insufficient
- All models stable over full time interval $\mathcal{T} = [0, T]$

Semi-Intrusive (Inferred) ROM

- Inferred models match or exceed projected counterparts
- Tensorial inference achieves best accuracy
- Demonstrates semi-intrusive approach viability

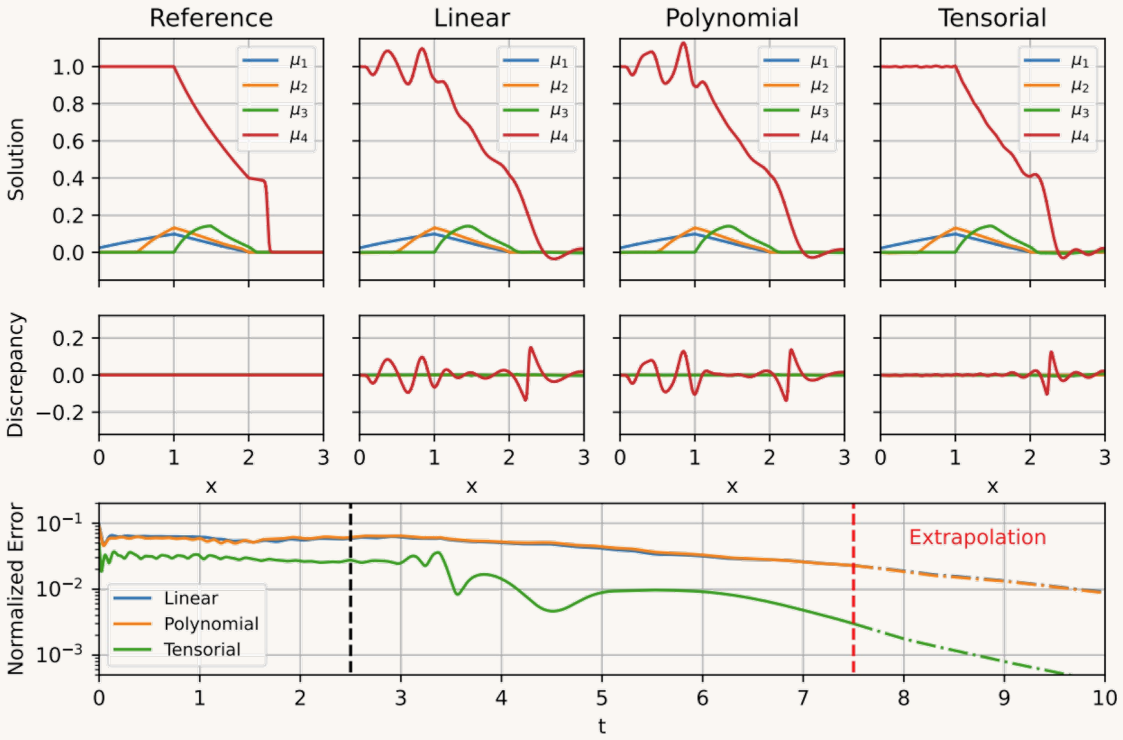

1D Convergence & Efficiency

Convergence vs. Latent Dimension

- Time-averaged $L^2(\mathcal{D}\times\mathcal{S}^2)$ error vs N_r (top): tensorial decays fastest
- Online speed-up vs N_r (bottom): all models achieve 10^2–$10^3\times$
- $N_r + N_q = 564$ fixed: trading latent for lifting dimensions
- Semi-intrusive inference ≥ projection for all N_r values

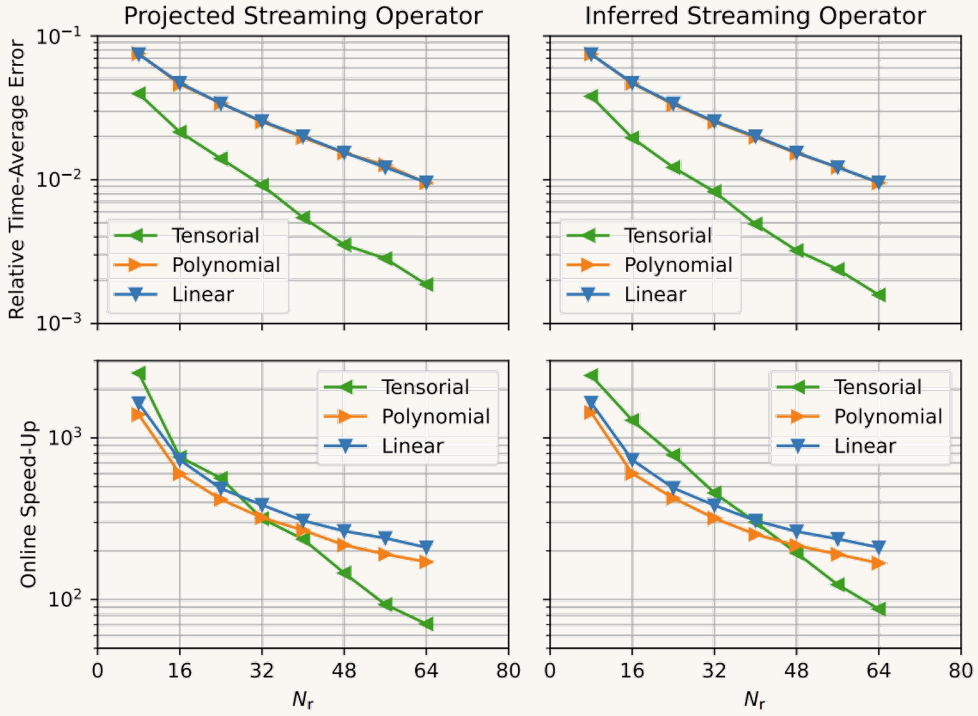

1D Lifting Dimension Study

Effect of Lifting Dimension (Latent Dimension Fixed)

- Increasing N_q: tensorial error drops orders of magnitude
- Element-wise & linear plateau early: limited by linear subspace quality
- Speed-up remains high $(10^2 – 10^3 \times)$ across all N_q values
- Tensorial: best accuracy-efficiency trade-off

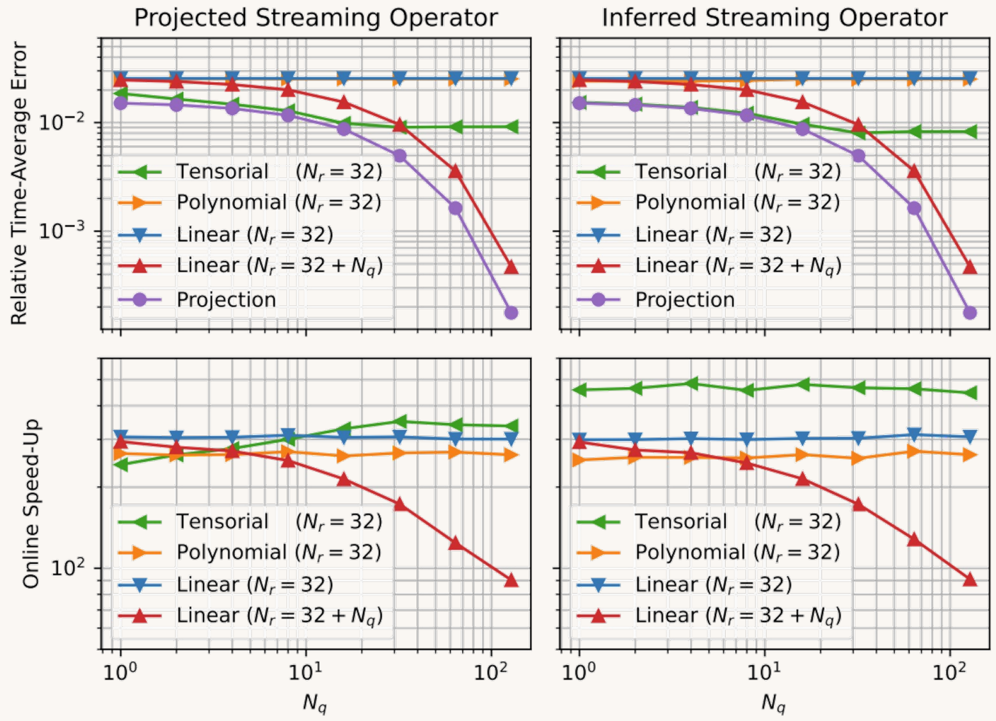

2D Benchmark: Heterogeneous Inclusions

2D Heterogeneous Configuration

- Domain: $\mathcal{D} = [0,7]^2$
- 12 material inclusions, 3 material types + background
- Solver: OpenSn (massively parallel, open-source)
- S_N quadrature: $N_\Omega = 32$ directions (level-symmetric)
- DG spatial: $N_{\boldsymbol{x}} = 21{,}840$ triangular cells
- Total DOF: $\mathcal{N} \approx 700{,}000$
- Time horizon: $T = 5,\ N_S = 1{,}000$ snapshots
- Full FOM solve: ~1 hour

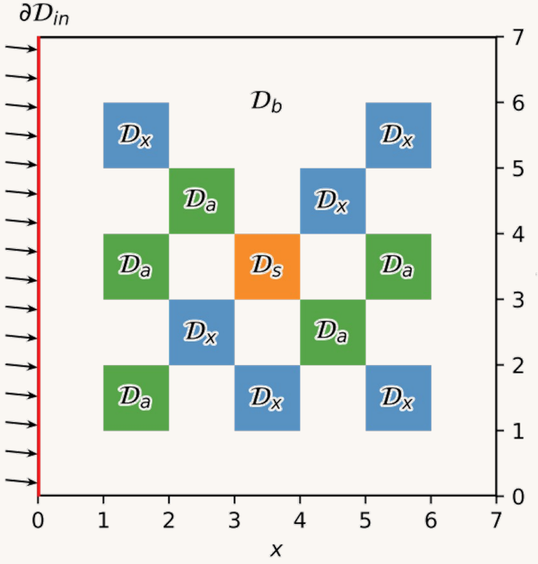

$$\sigma_t(\mathbf{x}) = \begin{cases} 1.00 & \mathbf{x} \in \mathcal{D}_a, \\ 1.00 & \mathbf{x} \in \mathcal{D}_x, \\ 1.00 & \mathbf{x} \in \mathcal{D}_s, \\ 0.00 & \mathbf{x} \in \mathcal{D}_b. \end{cases} \qquad \sigma_s(\mathbf{x}) = \begin{cases} 0.00 & \mathbf{x} \in \mathcal{D}_a, \\ 1.96 & \mathbf{x} \in \mathcal{D}_x, \\ 0.75 & \mathbf{x} \in \mathcal{D}_s, \\ 0.00 & \mathbf{x} \in \mathcal{D}_b. \end{cases}$$

2D Scalar Flux Evolution

Scalar Flux: $\boldsymbol{\Phi}(\boldsymbol{x}, t) = \int_{\mathcal{S}^2} \boldsymbol{\Psi}(\boldsymbol{x}, \boldsymbol{\Omega}, t)\, \mathrm{d}\boldsymbol{\Omega}$

- Neutron front propagates from left boundary through heterogeneous medium
- Inclusions create scattering and absorption shadows
- Solution is sharply structured in angle and space (challenging for linear ROMs)

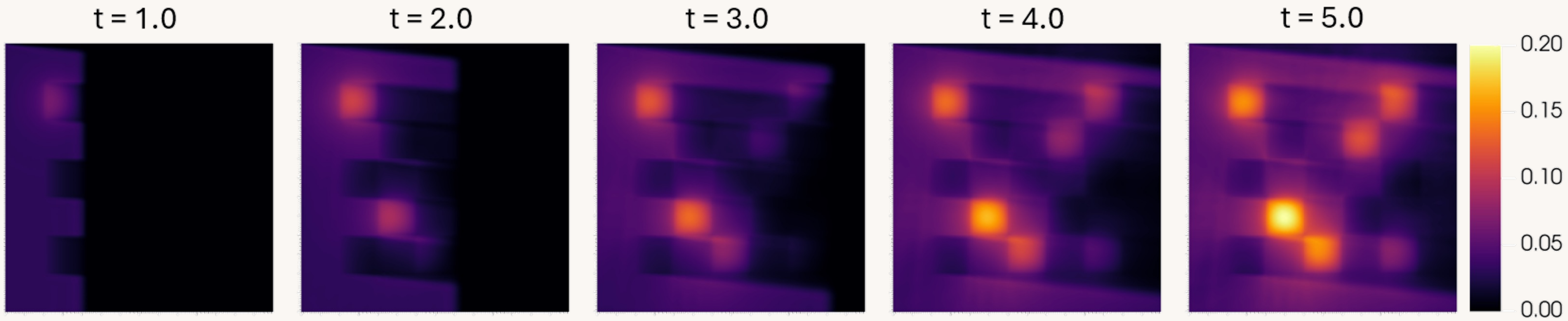

2D Results: Accuracy & Efficiency

2D Results: Accuracy & Speed-Up

- Tensor error up to one order lower than linear
- Convergence vs dimensions: stagnation at $N_r \approx 28 - 32$
- Semi-intrusive avoids global matrix assembly
- Online speed-up: 10^4– $10^5\times$ relative to OpenSn FOM
- In absolute terms: $700{,}000 \rightarrow 80$ DOFs and ~1 hr → ~0.036 s

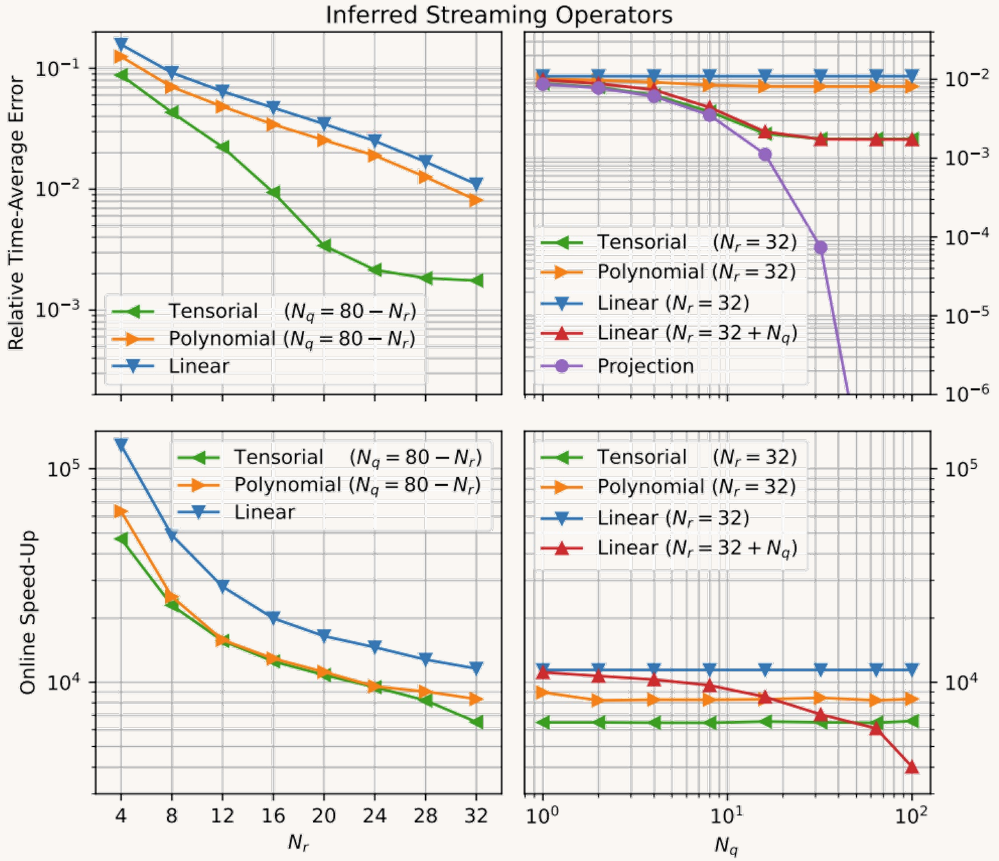

Outline

I. Motivation & Problem Setting

- Why ROM for parametric neutron transport?
- The parametric mono-energetic neutron transport problem
- Full order DG-S_N semi-discretization

II. Methodology

- Linear and Nonlinear Manifold ROM
- Proper orthogonal decomposition
- Nonlinear manifolds via quadratic lifting
- Semi-intrusive operator inference

III. Numerical Results

- 1D slab benchmark – projection & inference
- 1D lifting dimension study
- 2D heterogeneous benchmark – scalar flux & convergence

IV. Conclusions & Future Work

Conclusions & Future Work

Summary of Contributions

- Semi-intrusive OpInf avoids global advection FOM matrix, scalable to large $\mathcal{N}$
- Tensorial nonlinear manifold outperforms linear and element-wise across all tests
- Inferred operators match or surpass projected counterparts
- Hyper-parameter tuning and model stability remain open problems
- 1D: $10^2 – 10^3\times$ speed-up with $\mathcal{N}\sim 6{,}000$ DOF
- 2D: $10^4 – 10^5\times$ speed-up with $\mathcal{N}\sim 700{,}000$ DOF

Conclusions & Future Work

Summary of Contributions

- Semi-intrusive OpInf avoids global advection FOM matrix, scalable to large $\mathcal{N}$
- Tensorial nonlinear manifold outperforms linear and element-wise across all tests
- Inferred operators match or surpass projected counterparts
- Hyper-parameter tuning and model stability remain open problems
- 1D: $10^2 – 10^3\times$ speed-up with $\mathcal{N} \sim 6{,}000$ DOF
- 2D: $10^4 – 10^5\times$ speed-up with $\mathcal{N} \sim 700{,}000$ DOF

Future Directions

- Parametric ROM for online UQ (varying $\sigma_t(\boldsymbol{\mu}), \sigma_s(\boldsymbol{\mu}), Q(\boldsymbol{\mu})$)
- Affine decomposition of parametric operators at ROM level
- Multi-group energy: coupled system of transport equations
- 3D geometries with unstructured tetrahedral meshes

Relevant Literature

The following works provide the context for our research:

[1] J. Barnett, C. Farhat, *Quadratic approximation manifold for mitigating the Kolmogorov barrier in nonlinear projection-based model order reduction*, Journal of Computational Physics 464, 2022

[2] R. Geelen, L. Balzano, S. Wright, K. Willcox, *Learning physics-based reduced-order models from data using nonlinear manifolds*, Chaos: An Interdisciplinary Journal of Nonlinear Science, 2024

[3] M. L. Adams, E. W. Larsen, *Fast iterative methods for discrete-ordinates particle transport calculations*, Progress in Nuclear Energy, 2002

[4] Y. Wang, J. C. Ragusa, *A high-order discontinuous Galerkin method for the SN transport equations on 2D unstructured triangular meshes*, Annals of Nuclear Energy, 2009

[5] D. Andrs, Z. Hardy, D. Hawkins, J. Morel, D. Q. D. Nguyen, J. C. Ragusa, *OpenSn: A massively parallel, open-source simulation environment for discrete ordinates radiation transport*, Computer Physics Communications, 2025

THANK YOU

Texas A&M University
Department of Nuclear Engineering

francesco.silva@tamu.edu